5946 *Inorg. Chem.* **2009**, *48*, 5946–5956
DOI: 10.1021/ic9002862

Inorganic Chemistry
Article

Synthesis, Crystal Structures, and Luminescent Properties of Phenoxo-Bridged Heterometallic Trinuclear Propeller- and Sandwich-Like Schiff-Base Complexes

Hailong Wang,[†,‡] Daopeng Zhang,[†,‡] Zhong-Hai Ni,[*,‡] Xiyou Li,[‡] Laijin Tian,[‡] and Jianzhuang Jiang[*,†,‡]

[†]*Department of Chemistry, University of Science and Technology Beijing, Beijing 100083, China, and*
[‡]*Department of Chemistry, Shandong University, Jinan 250100, China*

Received February 11, 2009

A series of phenoxo-bridged heterometallic Schiff-base trinuclear complexes Zn−M−Zn [M = Cd(II), Pb(II), Nd(III), Eu(III), Gd(III), Tb(III), and Dy(III)] have been synthesized by a rational structural design based on two symmetrical Schiff-base ligands *N*,*N*′-bis(3-methoxysalicylidene)propylene-1,3-diamine (H_2L^a) and *N*,*N*′-bis(3-methoxysalicylidene)benzene-1,2-diamine (H_2L^b). Single X-ray diffraction analysis reveals a similar molecular structure among the eight propeller-like and seven sandwich-type phenoxo-bridged Zn−M−Zn complexes. In the compounds Cd[Zn(L^a)Cl]$_2$ (**1**), {Cd[Zn(L^b)Cl]$_2$}·H_2O (**2**), {Pb[Zn(L^b)Cl]$_2$}·$2H_2O$ (**4**), {Nd[Zn(L^a)Cl]$_2$(H_2O)}·$0.5ZnCl_4$·$2H_2O$ (**5**), and{M^{III}[Zn(L^a)Cl]$_2$(H_2O)}·$0.5ZnCl_4$·2MeOH [M = Eu(**7**), Gd (**9**), Tb (**11**), and Dy (**13**)], two $[Zn(L)Cl]^-$ units coordinate to the central metal ion as a tetradentate ligand using its four oxygen atoms, forming a two-blade propeller-like left-handed and right-handed chiral Zn−M−Zn configuration despite the racemic nature of the whole complexes. Compounds {Pb[Zn(L^a)Cl]$_2$}·MeOH (**3**), {Nd[Zn(L^b)Cl]$_2$(DMF)(OAc)}·CH_3CN (**6**), {Eu[Zn(L^b)Cl]$_2$(DMF)(OAc)}·CH_3CN (**8**), {Gd[Zn(L^b)Cl]$_2$(DMF)$_2$}·Cl·$2H_2O$ (**10**), {Tb[Zn(L^b)Cl]$_2$(DMF)$_2$}·Cl·$2H_2O$ (**12**), {Dy[Zn(L^b)Cl]$_2$(DMF)$_2$}·Cl·$2H_2O$ (**14**), and {Pb[Zn(L^b)Cl]$_2$}·$2H_2O$ (**15**) exhibit a relatively rare sandwich-type structure with a central metal ion clamped by two $[Zn(L)Cl]^-$ units. Photophysical studies indicate that all of the complexes exhibit luminescence both in solution and in solid sate, and there exists an energy transfer from the $[Zn(L)Cl]^-$ unit to the central rare earth ions of Nd(III) (**5** and **6**), Tb(III) (**11**), and Dy(III) (for **13**). In particular, systematic and comparative investigation of the photophysical properties of these trinuclear complexes reveals that the luminescence properties could easily be tuned by changing the central metal or the Schiff-base ligand.

Introduction

The metal complexes containing *N*,*N*′-bis(salicylidene) ethylenediamine (salen) derivatives were extensively studied within the fields of homogeneous catalysis,[1] nonlinear optics,[2] magnetics,[3] and biological metalloenzymes mimics.[4] Particularly, heterometallic Schiff-base complexes have attracted much more attention due to their intriguing properties arising from different meal ions.[5] In general, this type of complexes can be obtained through rational design and selection of an appropriate metal ion, Schiff-base ligand, bridging group, and balanced ion using the step-by-step method.[6] The salen-type ligands formed from 2,6-diformyl-4-methylphenol and diamines with two N_2O_2 cavities or one N_2O_2 and one O_4 cavity accommodating different metal ions have been extensively investigated over the past three

*To whom correspondence should be addressed. E-mail: jzjiang@sdu.edu.cn (J.J.).

(1) (a) Wezenberg, S. J.; Kleij, A. W. *Angew. Chem., Int. Ed.* **2008**, *47*, 2354. (b) Jain, S.; Zheng, X.; Jones, C. W.; Weck, M.; Davis, R. J. *Inorg. Chem.* **2007**, *46*, 8887. (c) Darensbourg, D. J.; Mackiewicz, R. M.; Phelps, A. L.; Billodeaux, D. R. *Acc. Chem. Res.* **2004**, *37*, 836. (d) McGarrigle, E. M.; Gilheany, D. G. *Chem. Rev.* **2005**, *105*, 1563. (e) Mazet, C.; Jacobsen, E. N. *Angew. Chem., Int. Ed.* **2008**, *47*, 1762.

(2) (a) Averseng, F.; Lacroix, P. G.; Malfant, I.; Lenoble, G.; Cassoux, P.; Nakatani, K.; Maltey-Fanton, I.; Delaire, J. A.; Aukauloo, A. *Chem. Mater.* **1999**, *11*, 995. (b) Rigamonti, L.; Demartin, F.; Forni, A.; Righetto, S.; Pasini, A. *Inorg. Chem.* **2006**, *45*, 10976. (c) Bella, S. D.; Fragala, I. *New J. Chem.* **2002**, *26*, 285.

(3) (a) Miyasaka, H.; Takahashi, H.; Madanbashi, T.; Sugiura, K.-i.; Clerac, R.; Nojiri, H. *Inorg. Chem.* **2005**, *44*, 5969. (b) Kim, J. I.; Yoo, H. S.; Koh, E. K.; Kim, H. C.; Hong, C. S. *Inorg. Chem.* **2007**, *46*, 8481. (c) Ni, Z.-H.; Kou, H.-Z.; Zhang, L.-F.; Ge, C.; Cui, A.-L.; Wang, R.-J.; Li, Y.; Sato, O. *Angew. Chem., Int. Ed.* **2005**, *44*, 7742. (d) Yuan, M.; Zhao, F.; Zhang, W.; Wang, Z.-M.; Gao, S. *Inorg. Chem.* **2007**, *46*, 11235.

(4) (a) Ueno, T.; Koshiyama, T.; Ohashi, M.; Kondo, K.; Kono, M.; Suzuki, A.; Yamane, T.; Watanabe, Y. *J. Am. Chem. Soc.* **2005**, *127*, 6556. (b) Yamami, M.; Furutachi, H.; Yokoyama, T.; Okawa, H. *Inorg. Chem.* **1998**, *37*, 6832. (c) Laskin, J.; Yang, Z.; Chu, I. K. *J. Am. Chem. Soc.* **2008**, *130*, 3218.

(5) (a) Sakamoto, M.; Manseki, K.; Okawa, H. *Coord. Chem. Rev.* **2001**, *219*, 379. (b) Branzea, D. G.; Sorace, L.; Maxim, C.; Andruh, M.; Caneschi, A. *Inorg. Chem.* **2008**, *47*, 6590. (c) Kahn, O.; Galy, J.; Journaux, Y.; Jaud, J.; Morgenstern-Badarau, I. *J. Am. Chem. Soc.* **1982**, *104*, 2165.

(6) Bencini, A.; Benelli, C.; Caneschi, A.; Carlin, R. L.; Dei, A.; Gatteschi, D. *J. Am. Chem. Soc.* **1985**, *107*, 8128.

 Published on Web 06/04/2009

decades. Recently, the compartmental salen-type ligands derived from the 2:1 condensation between 3-methoxysalicylaldehyde and diamines provide two dissimilar N_2O_2 and O_4 cavities to bind two different metal ions bridged by phenoxo oxygen atoms, leading to interesting magnetic phenomena and intriguing optic properties.[7,8] A new salen-type system developed by Nabeshima and co-workers was revealed to exhibit excellent selectivity in the guest recognition area.[9] However, to the best of our knowledge, any report of the luminescence properties of Schiff-base heterometallic trinuclear complexes remains rare.[10]

The salen-type complexes of Zn(II) were revealed to display quite excellent optic properties, which can effectively transfer energy to the second metal ion, such as a rare earth ion.[8,11] As a result, in the present paper, the Zn(II) ion was chosen as the first metal ion to coordinate with Schiff-base ligand *N*,*N*′-bis(3-methoxysalicylidene)propylene-1, 3-diamine (H_2L^a) with a relatively flexible structure and *N*, *N*′-bis(3-methoxysalicylidene)benzene-1,2-diamine (H_2L^b) with a relatively rigid structure, Chart 1. On the basis of these two Schiff-base mononuclear Zn(II) complexes, a series of 15 new phenoxo-bridged heterometallic trinuclear compounds including $Cd[Zn(L^a)Cl]_2$ (**1**), $\{Cd[Zn(L^b)Cl]_2\}\cdot H_2O$ (**2**), $\{Pb[Zn(L^a)Cl]_2\}\cdot MeOH$ (**3**), $\{Pb[Zn(L^b)Cl]_2\}\cdot 2H_2O$ (**4**), $\{Nd[Zn(L^a)Cl]_2(H_2O)\}\cdot 0.5ZnCl_4\cdot 2H_2O$ (**5**), $\{Nd[Zn(L^b)Cl]_2(DMF)(OAc)\}\cdot CH_3CN\cdot$(**6**), $\{Eu[Zn(L^a)Cl]_2(H_2O)\}\cdot 0.5ZnCl_4\cdot 2MeOH$ (**7**), $\{Eu[Zn(L^b)Cl]_2(DMF)(OAc)\}\cdot CH_3CN$ (**8**), $\{Gd[Zn(L^a)Cl]_2(H_2O)\}\cdot 0.5ZnCl_4\cdot 2MeOH$ (**9**), $\{Gd[Zn(L^b)Cl]_2(DMF)_2\}\cdot Cl\cdot 2H_2O$ (**10**), $\{Tb[Zn(L^a)Cl]_2(H_2O)\}\cdot 0.5ZnCl_4\cdot 2MeOH$ (**11**), $\{Tb[Zn(L^b)Cl]_2(DMF)_2\}\cdot Cl\cdot 2H_2O$ (**12**), $\{Dy[Zn(L^a)Cl]_2(H_2O)\}\cdot 0.5ZnCl_4\cdot 2MeOH$ (**13**), $\{Dy[Zn(L^b)Cl]_2(DMF)_2\}\cdot Cl\cdot 2H_2O$ (**14**), and $\{Pb[Zn(L^b)Cl]_2\}\cdot 2H_2O$ (**15**) have been rationally designed, synthesized, and characterized by single-crystal X-ray diffraction, IR, and elemental analysis. The luminescence properties of these complexes, **1**−**14**, were systematically investigated.

Experimental Section

General Details. All solvents and metal salts were used as received without further purification. Solvents for photophysical studies were dried in molecular sieves and freshly distilled under dry nitrogen gas before use. Fluorescence spectra were measured on a multifrequency phase and modulation fluorometer in DMSO solution and in the solid state. IR spectra were recorded on a Nicolet IR 200 FTIR spectrometer in the 4000−400 cm^{-1} region. Elemental analyses were carried out with an Elementary Vario El.

Chart 1

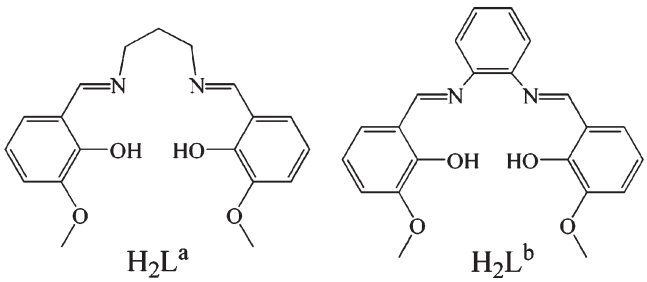

Single-Crystal X-Ray Diffraction Determination. Crystal data for all 15 complexes were collected on a Bruker SMART APEXII CCD diffractometer with graphite monochromatic Mo Kα radiation ($\lambda = 0.71073$ Å) using the SMART and SAINT programs at 298 K, and the structures were solved by the direct method (SHELXS-97) and refined by full-matrix least-squares (SHELXL-97) on F^2. Anisotropic thermal parameters were used for the nonhydrogen atoms and isotropic parameters for the hydrogen atoms. Hydrogen atoms were added geometrically and refined using a riding model. Crystallographic data and other pertinent information for all of the complexes are summarized in Tables 1 (for complexes **1**−**7**), 2 (for complexes **8**−**14**), and S1 (for complex **15**; Supporting Information). Selected bond distances and bond angles with their estimated standard deviations are listed in Tables 3 (for complexes **1**−**4**, **9**, **10**, and **15**) and S2 (for complex **5**−**8** and **11**−**14**; Supporting Information). CCDC 719711 for **1**; CCDC 719714−719716 for complexes **2**−**4**; CCDC 719717 for **15**; CCDC 719718−719721 for **9**, **10**, **5**, and **7**; CCDC 719712 and 719713 for **11** and **13**; and CCDC 730929−730932 for **8**, **6**, **12**, and **14** contain the supplementary crystallographic data for this paper. These data can be obtained free of charge from the Cambridge Crystallographic Data Centre via www.ccdc.cam.ac.uk/data_request/cif.

Synthesis of Precursors H_2L^a, H_2L^b, ZnL^a, and ZnL^b. The Schiff-base ligands H_2L^a and H_2L^b were obtained from the reaction between 3-methoxysalicylaldehyde and the corresponding diamine according to the reported procedure[12] and react with $Zn(OAc)_2\cdot 2H_2O$ (1:1 molar ratio) in methanol and ethanol, respectively, providing corresponding zinc complexes ZnL^a and ZnL^b.[13] It is worth noting that the former compound, ZnL^a, was used without being separated from the yellow mother solution. This is also true for ZnL^b, used to synthesize complexes **6**, **8**, **10**, **12**, and **14**.

For complex ZnL^a, IR (cm^{-1}, KBr): 1628 (s, $\nu_{C=N}$), 1220 (s, ν_{C-N}), 738 (m, γ_{C-H}).

For complex ZnL^b, IR (cm^{-1}, KBr): 1613 (s, $\nu_{C=N}$), 1237 (s, ν_{C-N}), 736 (m, γ_{C-H}).

Synthesis of $Cd(ZnL^a)_2Cl_2$ (1). A mixture of metal-free Schiff-base ligand H_2L^a (0.4 mmol 0.1368 g) and $Zn(OAc)_2\cdot 2H_2O$ (0.4 mmol 0.0878 g) in methanol (20 mL) was stirred for 30 min at room temperature. Then, a solution of $CdCl_2\cdot 2.5H_2O$ (0.2 mmol 0.0457 g) in methanol was added dropwise, and the mixture was kept stirring for another 30 min at room temperature. After being filtered, the reaction solution was put into the fridge to allow for solvent evaporation at 5 °C for one week, providing yellow single crystals at a yield of 0.095 g, 48%. IR (cm^{-1}, KBr): 1626 (s, $\nu_{C=N}$),

(7) (a) Margeat, O.; Lacroix, P. G.; Costes, J. P.; Donnadieu, B.; Lepetit, C. *Inorg. Chem.* **2004**, *43*, 4743. (b) Costes, J.-P.; Shova, S.; Wernsdorfer, W. *Dalton Trans.* **2008**, 1843. (c) Fellah, F. Z. C.; Costes, J.-P.; Dahan, F. *Inorg. Chem.* **2008**, *47*, 6444.

(8) (a) Yang, X.-P.; Jones, R. A.; Wong, W.-K.; Lynch, V.; Oyec, M. M.; Holmes, A. L. *Chem. Commun.* **2006**, 1836. (b) Yang, X.-P; Jones, R. A.; Lynch, V.; Oyeb, M. M.; Holmesb, A. L. *Dalton Trans.* **2005**, 849. (c) Wong, W.-K.; Yang, X.-P.; Jones, R. A.; Rivers, J. H.; Lynch, V.; Lo, W.-K.; Xiao, D.; Oye, M. M.; Holmes, A. L. *Inorg. Chem.* **2006**, *45*, 4340.

(9) (a) Akine, S.; Nabeshima, T. *Inorg. Chem.* **2005**, *44*, 1205. (b) Akine, S.; Matsumoto, T.; Taniguchi, T.; Nabeshima, T. *Inorg. Chem.* **2005**, *44*, 3270. (c) Akine, S.; Taniguchi, T.; Nabeshima, T. *Angew. Chem., Int. Ed.* **2002**, *41*, 24.

(10) (a) Chandrasekhar, V.; Azhakar, R.; Zacchini, S.; Bickley, J. F.; Steiner, A. *Inorg. Chem.* **2005**, *44*, 4608. (b) Chandrasekhar, V.; Azhakar, R.; Bickley, J.; Steiner, A. *Chem. Commun.* **2005**, 459. (c) You, Z.-L.; Zhu, H.-L.; Liu, W.-S. *Z. Anorg. Allg. Chem.* **2004**, *630*, 1617. (d) Chakraborty, J.; Thakurta, S.; Samanta, B.; Ray, A.; Pilet, G.; Batten, S. R.; Jensen, P.; Mitra, S. *Polyhedron* **2007**, *26*, 5139.

(11) (a) Ma, Y.; Chao, H.-Y.; Wu, Y.; Lee, S. T.; Yu, W.-Y.; Che, C.-M. *Chem. Commun.* **1998**, 2491. (b) Mizukami, S.; Houjou, H.; Nagawa, Y.; Kanesato, M. *Chem. Commun.* **2003**, 1148. (c) Escudero-Adán, E. C.; Benet-Buchholz, J.; Kleij, A. W. *Inorg. Chem.* **2008**, *47*, 4256. (d) Lo, W.-K.; Wong, W.-K.; Wong, W.-Y.; Guo, J. *Eur. J. Inorg. Chem.* **2005**, 3950.

(12) Costes, J.-P.; Dahan, F.; Dupuis, A. *Inorg. Chem.* **2000**, *39*, 165.

(13) Lo, W.-K.; Wong, W.-K.; Guo, J.; Wong, W.-Y.; Li, K.-F.; Cheah, K.-W. *Inorg. Chim. Acta* **2004**, *357*, 4510.

Table 1. Crystal Data and Structure Refinement for Complexes 1–7

compound	1	2	3	4	5	6	7
molecule formula	$C_{38}H_{40}CdCl_2N_4O_8Zn_2$	$C_{44}H_{38}CdCl_2N_4O_9Zn_2$	$C_{39}H_{44}Cl_2N_4O_9PbZn_2$	$C_{44}H_{40}Cl_2N_4O_{10}PbZn_2$	$C_{38}H_{44}Cl_4N_4NdO_{11}Zn_{2.5}$	$C_{51}H_{49}Cl_2NdN_6O_{11}Zn_2$	$C_{40}H_{50}Cl_4EuN_4O_{11}Zn_{2.5}$
cryst syst	monoclinic	monoclinic	monoclinic	monoclinic	orthorhombic	triclinic	orthorhombic
space group	$P2_1/c$	$P2_1/c$	$P2_1/c$	$P2_1/c$	*Pbcn*	$P\bar{1}$	*Pbcn*
a (Å)	19.1860(17)	13.148(3)	17.6600(19)	13.265(15)	14.150(5)	11.3522(9)	14.0696(8)
b (Å)	8.9947(8)	25.385(6)	12.7070(13)	25.83(3)	18.861(5)	12.5604(9)	18.8662(10)
c (Å)	23.430(2)	16.826(4)	19.278(2)	17.31(2)	35.694(5)	19.3649(14)	35.6616(19)
α (deg)	90.00	90.00	90.00	90	90.00	81.7360(10)	90.00
β (deg)	99.216(10)	110.160(9)	100.620(5)	112.04(2)	90.00	80.5030(10)	90.00
γ (deg)	90.00	90.00	90.00	90.00	90.00	69.1370(10)	90.00
V (Å^3)	3991.2(6)	5272(2)	4252.0(8)	5498(11)	9526(4)	2534.0(3)	9466.0(9)
Z	4	4	4	4	8	2	8
D_{calcd} (g cm^{-3})	1.656	1.362	1.752	1.442	2.600	1.662	1.712
F(000)	2008	2176	2216	2352	4727	1278	4896
θ (deg)	1.08, 25.00	1.89, 25.00	1.17, 26.00	1.58, 25.00	1.80, 25.00	1.07, 25.00	1.14, 27.50
R_1 ($I > 2\sigma(I)$)	0.0307,	0.1001	0.0480	0.0990	0.0645	0.0249	0.0322
wR_2 ($I > 2\sigma(I)$)	0.0755	0.2009	0.1055	0.2206	0.1680	0.0657	0.0678
S	1.042	0.810	0.998	0.830	1.041	1.049	1.004

1220 (s, ν_{C-N}), 739 (m, γ_{C-H}). Anal. calcd for $C_{38}H_{40}CdCl_2N_4O_8Zn_2$ (M = 994.88): C, 45.88; H, 4.05; N, 5.63. Found: C, 45.56; H, 3.99, N, 5.59.

Synthesis of $[Cd(ZnL^b)_2Cl_2]\cdot H_2O$ (2). A mixture containing ZnL^b (0.2 mmol, 0.0880 g) and $CdCl_2\cdot 2.5H_2O$ (0.1 mmol, 0.0228 g) in DMSO (25 mL) was refluxed until the solution became clear and was then cooled down to room temperature and filtered. Microcrystals were obtained by putting the filtrate in the air. Alternatively, perfect yellow single crystals were obtained by diffusing diethyl ether into the filtrate. Yield: 0.049 g, 45%. IR (cm^{-1}, KBr): 1613 (s, $\nu_{C=N}$), 1237 (s, ν_{C-N}), 747 (m, γ_{C-H}). Anal. calcd for $C_{44}H_{38}CdCl_2N_4O_9Zn_2$ (M = 1080.93): C, 48.89; H, 3.54; N, 5.18. Found: C, 48.73; H, 3.34; N, 5.10.

Synthesis of $[Pb(ZnL^a)_2Cl_2]\cdot MeOH$ (3). By employing the above-described procedure used to prepare complex **1**, with $PbCl_2$ (0.2 mmol, 0.0556 g) instead of $CdCl_2\cdot 2.5H_2O$ as a starting material, yellow single crystals of complex **3** were obtained at a yield of 0.085 g, 38%. IR (cm^{-1}, KBr): 1624 (s, $\nu_{C=N}$), 1219 (s, ν_{C-N}), 734 (m, γ_{C-H}). Anal. calcd for $C_{39}H_{44}Cl_2N_4O_9PbZn_2$ (M=1121.71): C, 41.76; H, 3.95; N, 4.99. Found: C, 41.55; H, 3.78; N, 4.89.

Synthesis of $[Pb(ZnL^b)_2Cl_2]\cdot 2H_2O$ (4) and $[Pb(ZnL^b)_2Cl_2]\cdot 2H_2O$ (15). A mixture of $PbCl_2$ (0.0278 g, 0.100 mmol) and ZnL^b (0.0880 g, 0.2 mmol) in a mixed solvent of DMF (25 mL) and H_2O (1 mL) was refluxed until the solution became clear, which was then cooled down to room temperature and filtered. Perfect yellow rectangle crystals of complex **4** were obtained by putting the filtrate in the air for one week. It is worth noting that, after filtering the yellow rectangle crystals of **4**, three yellow crystals of complex **15** with a polyhedron shape were obtained from the remaining filtrate after putting it in the air for a further week, as a byproduct of **4**. Yield: 0.069 g, 29% for complex **4**. IR (cm^{-1}, KBr): 1611 (s, $\nu_{C=N}$), 1230 (s, ν_{C-N}), 741 (m, γ_{C-H}). Anal. calcd for $C_{44}H_{40}Cl_2N_4O_{10}PbZn_2$ (M = 1193.73): C, 44.27; H, 3.78; N, 4.69. Found: C, 44.17; H, 3.54; N, 4.58.

Synthesis of $\{Nd[Zn(L^a)Cl]_2(H_2O)\}_2\cdot ZnCl_4\cdot 4H_2O$ (5). The method was similar to that used for preparing **1**. A mixture of H_2L^a (0.1368 g, 0.4 mmol) and $Zn(OAc)_2\cdot 2H_2O$ (0.0876 g, 0.4 mmol) in methanol (30 mL) was kept stirring for 30 min; then, a solution of $NdCl_3\cdot 6H_2O$ (0.0717 g, 0.2 mmol) in methanol was added. After reaction for another 30 min, the reaction mixture was filtered. Crystals suitable for X-ray diffraction analysis were obtained by allowing the filtrate to slowly evaporate at 5 °C in the fridge, with a yield of 0.111 g, 48%. IR (cm^{-1}, KBr): 1628 (s, $\nu_{C=N}$), 1220 (s, ν_{C-N}), 738 (m, γ_{C-H}). Anal. calcd for $C_{38}H_{44}Cl_4NdN_4O_{11}Zn_{2.5}$ (M = 1182.35): C, 38.54; H, 3.91; N, 4.73. Found: C, 38.45; H, 3.76; N, 4.64.

Synthesis of $\{Nd[Zn(L^b)Cl]_2(DMF)(OAc)\}\cdot CH_3CN$ (6). A mixture of H_2L^b (0.0752 g, 0.2 mmol) and $Zn(OAc)_2\cdot 2H_2O$ (0.0440 g, 0.2 mmol) in 15 mL of acetonitrile/DMF (1:1) was kept refluxing for 5 min; then, a solution of $NdCl_3\cdot 6H_2O$ (0.0358 g, 0.1 mmol) in DMF was added. After the solution became clear, the reaction solution was then cooled down to room temperature and filtered. Perfect yellow crystals of complex **6** for X-ray diffraction analysis were obtained by slowly diffusing diethyl ether into the filtrate, with a yield of 0.054 g, 43%. IR (cm^{-1}, KBr): 1652 (s, $\nu_{C=O}$), 1613 (s, $\nu_{C=N}$), 1236 (s, ν_{C-N}), 737 (m, γ_{C-H}). Anal. calcd for $C_{51}H_{49}Cl_2NdN_6O_{11}Zn_2$ (M = 1267.93): C, 48.31; H, 3.90; N, 6.63. Found: C, 48.35; H, 3.86; N, 6.64.

Synthesis of Complexes $Eu[Zn(L^a)Cl]_2(H_2O)\cdot 0.5ZnCl_4\cdot 2MeOH$ (7), $[Gd(ZnL^a)_2Cl_2\cdot H_2O]\cdot 0.5ZnCl_4\cdot 2MeOH$ (9), $Tb[Zn(L^a)Cl]_2(H_2O)\cdot 0.5ZnCl_4\cdot 2MeOH$ (11), and $Dy[Zn(L^a)Cl]_2\cdot H_2O\cdot 0.5ZnCl_4\cdot 2MeOH$ (13). By using the above-mentioned procedure employed to prepare complex **5**, with $EuCl_3\cdot 6H_2O$ (0.0733 g, 0.2 mmol), $GdCl_3\cdot 6H_2O$ (0.0744 g, 0.2 mmol), $TbCl_3\cdot 6H_2O$ (0.0747 g, 0.2 mmol), or $DyCl_3\cdot 6H_2O$ (0.0754 g,

Table 2. Crystal Data and Structure Refinement for Complexes **8**–**14**

compound	**8**	**9**	**10**	**11**	**12**	**13**	**14**
molecule formula	$C_{51}H_{49}Cl_2EuN_6O_{11}Zn_2$	$C_{40}H_{50}Cl_4GdN_4O_{11}Zn_{2.5}$	$C_{50}H_{54}Cl_3GdN_6O_{12}Zn_2$	$C_{40}H_{50}Cl_4TbN_4O_{11}Zn_{2.5}$	$C_{50}H_{52}Cl_3N_6O_{12}TbZn_2$	$C_{40}H_{50}Cl_4DyN_4O_{11}Zn_{2.5}$	$C_{50}H_{52}Cl_3N_6O_{12}DyZn_2$
cryst syst	triclinic	orthorhombic	monoclinic	orthorhombic	monoclinic	orthorhombic	monoclinic
space group	$P\bar{1}$	*Pbcn*	$P2_1/n$	*Pbcn*	$P2_1/n$	*Pbcn*	$P2_1/n$
a (Å)	11.2510(8)	14.0765(7)	11.409(2)	14.065(3)	11.418(2)	14.0654(8)	11.353(2)
b (Å)	12.6031(9)	18.8454(10)	33.1030(16)	18.807(4)	32.990(6)	18.7986(11)	33.003(5)
c (Å)	19.4240(14)	35.6295(18)	15.8110(15)	35.632(7)	15.814(3)	35.664(2)	15.775(3)
α (deg)	81.6470(10)	90.00	90.00	90.00	90	90.00	90
β (deg)	80.5300(10)	90.00	106.986(2)	90.00	108.075(3)	90.00	107.937(3)
γ (deg)	68.8300(10)	90.00	90.00	90.00	90	90.00	90
V (Å^3)	2522.3(3)	9451.7(8)	5710.9(12)	9425(3)	5663.0(18)	9429.9(9)	5623.3(17)
Z	2	8	4	8	4	8	4
D_{calcd} (g cm^{-3})	1.679	1.722	1.541	1.729	1.554	1.734	1.572
F(000)	1284	4904	2668	4912	2664	4920	2676
θ (deg)	1.74, 25.00	1.81, 26.50	1.82, 26.50	1.81, 27.52	1.23, 27.62	1.14, 25.00	1.83, 25.00
R_1 ($I > 2\sigma(I)$)	0.0298	0.0311	0.0821	0.0327	0.0641	0.0278	0.0740,
wR_2 ($I > 2\sigma(I)$)	0.0747	0.0650	0.2172	0.0692	0.1884	0.0628	0.2001
S	0.966	1.055	1.017	1.042	1.095	1.041	0.970

0.2 mmol) employed instead of $NdCl_3 \cdot 6H_2O$ as a starting material, perfect crystals of complexes **7**, **9**, **11**, and **13** were obtained.

For complex **7**, yield: 0.141 g, 58%. IR (cm^{-1}, KBr): 1629 (m, $\nu_{C=N}$), 1221 (s, ν_{C-N}), 732 (m, γ_{C-H}). Anal. calcd for $C_{40}H_{50}Cl_4EuN_4O_{11}Zn_{2.5}$ (M = 1220.14): C, 39.37; H, 4.13; N, 4.59. Found: C, 39.35; H, 4.06; N, 4.54.

For complex **9**, yield: 0.105 g, 43%. IR (cm^{-1}, KBr): 1628 (s, $\nu_{C=N}$), 1221 (s, ν_{C-N}), 738 (m, γ_{C-H}). Anal. calcd for $C_{40}H_{50}Cl_4GdN_4O_{11}Zn_{2.5}$ (M = 1225.43): C, 39.20; H, 4.11; N, 4.57. Found: C, 39.02; H, 4.10; N, 4.48.

For complex **11**, yield: 0.0863 g, 35%. IR (cm^{-1}, KBr): 1631 (s, $\nu_{C=N}$), 1226 (s, ν_{C-N}), 745 (m, γ_{C-H}). Anal. calcd for $C_{40}H_{50}Cl_4TbN_4O_{11}Zn_{2.5}$ (M = 1227.10): C, 39.15; H, 4.11; N, 4.57. Found: C, 39.08; H, 3.98; N, 4.43.

For complex **13**, yield: 0.135 g, 55%. IR (cm^{-1}, KBr): 1628 (s, $\nu_{C=N}$), 1220 (s, ν_{C-N}), 738 (m, γ_{C-H}). Anal. calcd for $C_{40}H_{50}Cl_4DyN_4O_{11}Zn_{2.5}$ (M = 1230.68): C, 39.04; H, 4.10; N, 4.55. Found: C, 38.98; H, 4.06; N, 4.47.

Synthesis of Complexes $\{Eu[Zn(L^b)Cl]_2(DMF)(OAc)\}\cdot CH_3CN$ (8), $[Gd(ZnL^b)_2Cl_2(DMF)_2]\cdot Cl\cdot 2H_2O$ (10), $\{Tb[Zn(L^b)Cl]_2(DMF)_2\}\cdot Cl\cdot 2H_2O$ (12), and $\{Dy[Zn(L^b)Cl]_2(DMF)_2\}\cdot Cl\cdot 2H_2O$ (14). By using the above-mentioned procedure employed to prepare complex **6**, with $EuCl_3 \cdot 6H_2O$ (0.0366 g, 0.1 mmol), $GdCl_3 \cdot 6H_2O$ (0.0372 g, 0.1 mmol), $TbCl_3 \cdot 6H_2O$ (0.0373 g, 0.1 mmol), or $DyCl_3 \cdot 6H_2O$ (0.0377 g, 0.1 mmol) employed instead of $GdCl_3 \cdot 6H_2O$ as a starting material, perfect crystals of complexes **8**, **10**, **12**, and **14** were obtained.

For complex **8**, yield: 0.047 g, 37%. IR (cm^{-1}, KBr): 1652 (s, $\nu_{C=O}$), 1613 (s, $\nu_{C=N}$), 1239 (s, ν_{C-N}), 740 (m, γ_{C-H}). Anal. calcd for $C_{51}H_{49}Cl_2EuN_6O_{11}Zn_2$ (M = 1275.66): C, 48.02; H, 3.87; N, 6.59. Found: C, 48.01; H, 3.86; N, 6.54.

For complex **10**, yield: 0.061 g, 46%. IR (cm^{-1}, KBr): 1614 (s, $\nu_{C=N}$), 1240 (s, ν_{C-N}), 737 (m, γ_{C-H}). Anal. calcd for $C_{50}H_{54}Cl_3GdN_6O_{12}Zn_2$ (M = 1325.42): C, 45.31; H, 4.11; N, 6.34. Found: C, 45.27; H, 4.03; N, 6.32.

For complex **12**, yield: 0.0411 g, 31%. IR (cm^{-1}, KBr): 1613 (s, $\nu_{C=N}$), 1241 (s, ν_{C-N}), 735 (m, γ_{C-H}). Anal. calcd for $C_{50}H_{54}Cl_3N_6O_{12}TbZn_2$ (M = 1327.10): C, 45.25; H, 4.10; N, 6.33. Found: C, 45.28; H, 4.08; N, 6.33.

For complex **14**, yield: 0.0679 g, 51%. IR (cm^{-1}, KBr): 1613 (s, $\nu_{C=N}$), 1241 (m, ν_{C-N}), 734 (m, γ_{C-H}). Anal. calcd for $C_{50}H_{54}Cl_3N_6O_{12}DyZn_2$ (M = 1330.67): C, 45.13; H, 4.09; N, 6.32. Found: C, 45.18; H, 4.03; N, 6.34.

Results and Discussion

Synthesis of Heterometallic Trinuclear Complexes Zn_2M. The metal-free Schiff-base ligands *N*,*N*′-bis(3-methoxysalicylidene)-propylene-1,3-diamine (H_2L^a) and *N*,*N*′-bis(3-methoxysalicylidene)benzene-1,2-diamine (H_2L^b) were prepared easily by the condensation reaction between *o*-vanillin and the corresponding diamine in a 2:1 molar ratio.[12] With the help of good selectivity of this type of Schiff-base ligand, the first metal Zn(II) ion entered readily into the N_2O_2 cavity of the H_2L^a or H_2L^b ligand, providing precursors ZnL^a and ZnL^b.[13] The open O_4 cavity is then able to accommodate the second metal ion. In this work, 15 propeller- or sandwich-like heterometallic trinuclear complexes with the same motif, Zn−M−Zn [M = Cd(II), Pb(II), Nd(III), Eu(III), Gd(III), Tb(III), and Dy(III)] have been designed and obtained in a step-by-step conception via assembling complex ZnL (L = L^a and L^b) with 0.5 equiv of $MCl_x \cdot nH_2O$. The molecular formulas are confirmed by elemental analyses and X-ray single-crystal diffraction analysis.

Table 3. Selected Bond Lengths (Å) and Angles (deg) of complexes **1**−**4**, **9**, **10**, and **15**

	1	**2**	**3**	**4**	**9**		**10**		**15**	
N(1)−Zn(1)	2.125(3)	2.106(12)	2.088(9)	2.113(18)	Zn(1)−N(1)	2.078(3)	N(1)−Zn(1)	2.068(9)	Zn(1)−N(1)	2.071(2)
N(2)−Zn(1)	2.096(3)	2.077(13)	2.092(9)	2.094(18)	Zn(1)−N(2)	2.054(3)	N(2)−Zn(1)	2.056(9)	Zn(1)−N(2)	2.080(2)
N(3)−Zn(2)	2.096(3)	2.118(13)	2.128(8)	2.105(18)	Zn(2)−N(3)	2.071(3)	N(3)−Zn(2)	2.084(9)	Zn(1)−O(2)	2.0061(16)
N(4)−Zn(2)	2.130(3)	2.102(14)	2.069(8)	2.122(16)	Zn(2)−N(4)	2.075(3)	N(4)−Zn(2)	2.063(9)	Zn(1)−O(3)	2.0090(17)
O(2)−Zn(1)	2.057(2)	2.023(10)	2.009(6)	2.086(14)	Zn(1)−O(2)	2.052(2)	O(2)−Zn(1)	2.008(7)	Zn(1)−Cl(1)	2.2754(8)
O(3)−Zn(1)	2.090(2)	2.030(10)	2.065(6)	1.995(16)	Zn(1)−O(3)	2.122(2)	O(3)−Zn(1)	2.051(7)	Pb(1)−O(1)	3.048(16)
O(6)−Zn(2)	2.062(2)	2.064(10)	2.073(6)	2.037(15)	Zn(2)−O(6)	2.061(2)	O(6)−Zn(2)	2.005(7)	Pb(1)−O(2)	2.5185(16)
O(7)−Zn(2)	2.066(2)	2.047(12)	2.036(6)	2.032(14)	Zn(2)−O(7)	2.104(2)	O(7)−Zn(2)	2.037(7)	Pb(1)−O(3)	2.4576(17)
Cl(1)−Zn(1)	2.268(1)	2.251(5)	2.277(3)	2.251(6)	Zn(1)−Cl(1)	2.286(1)	Zn(1)−Cl(1)	2.258(4)	Pb(1)−O(4)	3.179 (17)
Cl(2)−Zn(2)	2.280(1)	2.243(5)	2.293(3)	2.274(7)	Zn(2)−Cl(2)	2.261(1)	Zn(2)−Cl(2)	2.246(4)		
O(1)−M	2.452(2)	2.638(12)	3.028(5)	2.782(15)	Gd(1)−O(1)	2.544(2)	O(1)−Gd(1)	2.758(8)		
O(2)−M	2.277(2)	2.262(10)	2.514(6)	2.458(15)	Gd(1)−O(2)	2.390(2)	O(2)−Gd(1)	2.358(7)		
O(3)−M	2.280(2)	2.230(10)	2.331(6)	2.532(12)	Gd(1)−O(3)	2.332(2)	O(3)−Gd(1)	2.378(8)		
O(4)−M	2.697(2)	2.646(12)	2.914(6)	2.763(12)	Gd(1)−O(4)	2.598(2)	O(5)−Gd(1)	2.665(8)		
O(5)−M	2.701(2)	2.561(12)	2.880(6)	2.739(15)	Gd(1)−O(5)	2.620(2)	O(6)−Gd(1)	2.318(7)		
O(6)−M	2.286(2)	2.280(10)	2.358(6)	2.454(15)	Gd(1)−O(6)	2.311(2)	O(7)−Gd(1)	2.394(7)		
O(7)−M	2.287(2)	2.278(11)	2.419(5)	2.527(15)	Gd(1)−O(7)	2.359(2)	O(9)−Gd(1)	2.321(9)		
O(8)−M	2.463(2)	2.668(11)	3.034(6)	2.802(15)	Gd(1)−O(8)	2.563(2)	O(10)−Gd(1)	2.282(8)		
					Gd(1)−O(9)	2.417(3)				
Zn(1)−O(2)−M	107.21(9)	104.9(4)	106.6(2)	103.6(7)	Zn(1)−O(2)−Gd(1)	106.7 (1)	Zn(1)−O(2)−Gd(1)	107.8(3)	Zn(1)−O(2)−Pb(1)	105.57(7)
Zn(1)−O(3)−M	105.99(9)	104.2(4)	111.6(2)	103.8(5)	Zn(1)−O(3)−Gd(1)	106.5 (1)	Zn(1)−O(3)−Gd(1)	105.6(3)	Zn(1)−O(3)−Pb(1)	107.71(7)
Zn(2)−O(6)−M	106.12(10)	103.1(5)	109.0(3)	106.3(6)	Zn(2)−O(6)−Gd(1)	112.3(1)	Zn(2)−O(6)−Gd(1)	108.5(3)	Zn(1A)−O(2A)−Pb(1)	105.57(7)
Zn(2)−O(7)−M	105.92(9)	102.6(5)	108.0(2)	103.9(6)	Zn(2)−O(7)−Gd(1)	108.9(1)	Zn(2)−O(7)−Gd(1)	104.7(3)	Zn(1A)−O(3A)−Pb(1)	107.71(7)

Scheme 1. Two Enantiomers A and B, Exhibiting a Two-Blade Propeller-Like Configuration, and Complex C, Possessing a Sandwich-Type Configuration

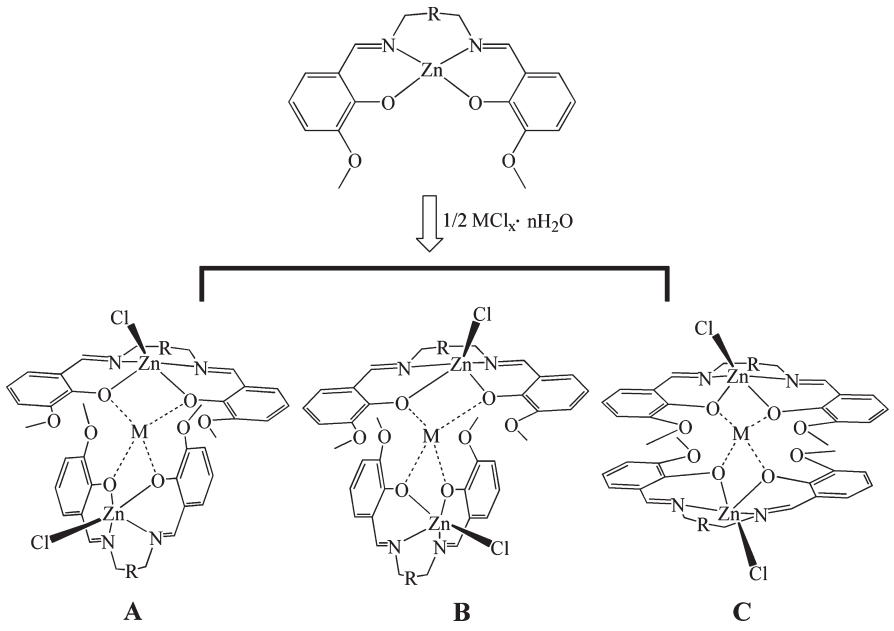

Interestingly, when a second metal ion was introduced, two crossed five-coordination achiral [Zn(L)Cl]$^-$ (L = L^a and L^b) units embraced the central metal ion, forming the chiral two-blade propeller-like left-handed and right-handed Zn−M−Zn configuration for compounds **1**, **2**, **4**, **5**, **7**, **9**, **11**, and **13**, Scheme 1. Such an intriguing outcome is determined by the inevitability of the crystallization procedure due to the following reasons: (1) Two ZnL (L = L^a and L^b) segments attached to the central M ion gives trinuclear moiety Zn−M−Zn (M = Cd, Pb, Nd, Eu, Gd, Tb, and Dy) with a propeller-like configuration possessing the C_{2v} symmetry. (2) The Zn(II) ion prefers a five-coordinated configuration and in turn locates slightly above the N_2O_2 plane of the Schiff-base ligand.[14] (3) The random attack of the chloride atom to the Zn(II) ion in each ZnL segment to balance the charge diminishes the symmetry of the trinuclear moiety to C_1 symmetry, leading to intrinsic chirality for the whole trinuclear moiety in nature. The left-handed and right-handed configurations were revealed by the X-ray molecular structure analysis results. The chirality of such trinuclear complexes is analogous to 1,1′-bi-2-naphthol derivatives but different from complexes based on achiral tripodal ligands.[15]

The seven other compounds, **3**, **6**, **8**, **10**, **12**, **14**, and **15**, were revealed to exhibit a sandwich-type configuration, Scheme 1, associated with a preference of the central metal ion and the coordination geometry of the organic ligand. It appears that the propeller-like molecular configuration is stabilized not only by the coordination interaction between the central metal ion and oxygen atoms of the Schiff-base ligand but also by the intramolecular hydrogen-bond interaction between the coordinated chloride atom and the methylic hydrogen atom of the Schiff-base ligand, with a Cl···H−C bond in the range of 3.474−3.825 Å. In a different manner, the intermolecular $\pi-\pi$ interaction between two coordinated Schiff-base ligands together with the coordination interaction around the central ions plays the key role in forming the sandwich configuration.

Crystal Structures of Cd(ZnL^a)$_2$Cl$_2$ (1) and [Cd(ZnL^b)$_2$Cl$_2$]·H$_2$O (2). The crystal structures of the two trinuclear Zn−Cd−Zn complexes are shown in Figure 1, and selected distances for **1** and **2** are summarized in Table 3. The crystallographic data reveal that both complexes constructed from different Schiff-base ligands crystallize in the same space group of $P2_1/c$, in which there exist similar neutral Cd[Zn(L)Cl]$_2$ units (L = L^a for **1** and L = L^b for **2**). In addition, the water molecules of crystallization are observed in **2**. All of the terminal Zn(II) ions in the two complexes exhibit a distorted square pyramidal geometry, with two nitrogen atoms and two oxygen atoms forming the basal plane and one chloride atom occupying the apical position. The Zn(II) ions of complexes **1** and **2** are separated with N_2O_2 planes of Schiff-base ligands, with an average distance of 2.854(2) and 2.933(12) Å. The Zn−Cl, Zn−O, and Zn−N bond lengths span the normal ranges of 2.243(4)−2.280(1), 2.023(10)−2.090(2), and 2.077(13)−2.130(3) Å, respectively.[16]

In the two complexes **1** and **2**, the central metal Cd(II) atom with an eight-coordinated mode is encapsulated in

(14) (a) Yang, X.-P.; Jones, R. A.; Wu, Q.-Y.; Oye, M. M.; Lo, W.-K.; Wong, W.-K.; Holmes, A. L. *Polyhedron*. **2006**, *25*, 271. (b) Wong, W.-K.; Liang, H.; Wong, W.-Y.; Cai, Z.; Li, K.-F.; Cheah, K.-W. *New J. Chem.* **2002**, *26*, 275. (c) Costes, J.-P.; Dahan, F.; Wernsdorfer, W. *Inorg. Chem.* **2006**, *45*, 5.

(15) (a) Cai, Y.-P.; Su, C.-Y.; Chen, C.-L.; Li, Y.-M.; Kang, B.-S.; Chan, A. S. C.; Kaim, W. *Inorg. Chem.* **2003**, *42*, 163. (b) Nakamura, H.; Sunatsuki, Y.; Kojima, M.; Matsumoto, N. *Inorg. Chem.* **2007**, *46*, 8170. (c) Yamada, T.; Shinoda, S.; Sugimoto, H.; Uenishi, J.-I.; Tsukube, H. *Inorg. Chem.* **2003**, *42*, 7932.

(16) (a) Chaudhuri, P.; Hess, M.; Muller, J.; Hildenbrand, K.; Bill, E.; Weyhermuller, T.; Wieghardt, K. *J. Am. Chem. Soc.* **1999**, *121*, 9599. (b) Neels, A.; Stoeckli-Evans, H. *Inorg. Chem.* **1999**, *38*, 6164. (c) Tang, Y.-Z.; Huang, X.-F.; Song, Y.-M.; Chan, H. *Inorg. Chem.* **2006**, *45*, 4868.

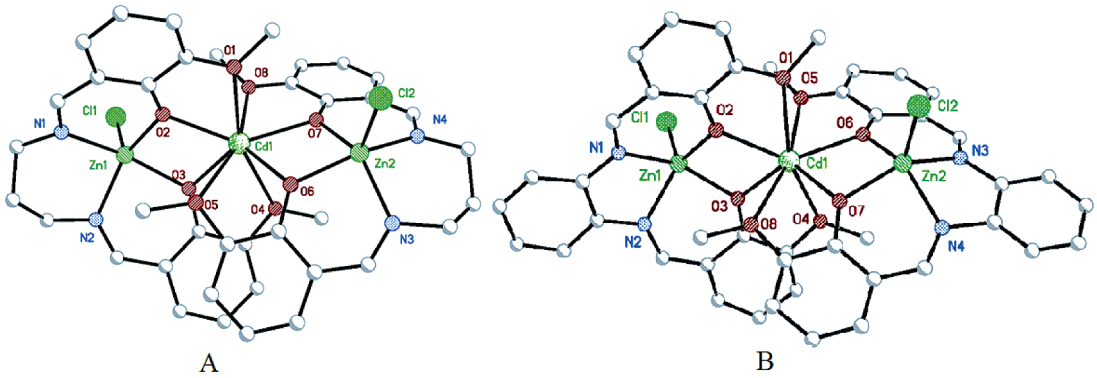

Figure 1. ORTEP drawings of the crystal structure in complexes **1** (A) and **2** (B), with all H atoms and solvent molecules omitted for clarity.

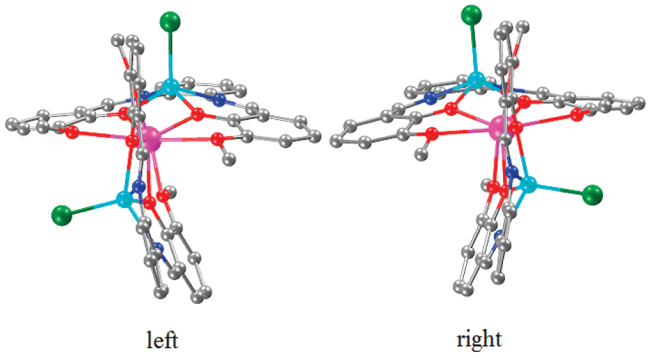

Figure 2. Structure diagram of two enantiomers in complex **2**.

the O_8 cavity formed by four oxygen atoms of bridging phenolic groups and another four from the methoxy groups of two ZnL (L = L^a and L^b) moieties connected to each other. The Cd−O bond distances are in the extensive range of 2.277(2)−2.701(2) Å for **1** and 2.278 (11)−2.668(11) Å for **2**, indicating interaction between the Cd(II) ion and the O atoms with different intensities.[11d] Two Zn(II) ions and a Cd(II) ion are nearly arranged in a line, with a Zn−M−Zn angle of 169.97 (9)° for **1** and 175.35(4)° for **2**. The two N_2O_2 planes of the Schiff base are crossed with dihedral angles of 67.38(9)° and 77.65(4)° for **1** and **2**, respectively. As shown in Figure 2 for **2** and Figure S1 for **1** (Supporting Information), two screwed five-coordinated Zn(II) segments, ZnL (L = L^a and L^b), embrace the central Cd(II) metal ion, forming the chiral two-blade propeller-like left-handed and right-handed Zn−M−Zn configuration. Unfortunately, both complexes **1** and **2** are racemate, in which the two enantiomers are not separated.

Crystal Structures of $[Pb(ZnL^a)_2Cl_2]\cdot MeOH$ (3), $[Pb(ZnL^b)_2Cl_2]\cdot 2H_2O$ (4), and $[Pb(ZnL^b)_2Cl_2]\cdot 2H_2O$ (15). The crystal structures of the three trinuclear Zn−Pb−Zn complexes **3**, **4**, and **15** are depicted in Figure 3, and selected bond lengths and angles for **3**, **4**, and **15** are listed in Table 3. In **3**, the Pb(II) ion is sandwiched between two $[Zn(L^a)Cl]^-$ moieties and locates in a distorted tetrahedron geometry formed by four phenolic oxygen atoms, with Pb−O distances varying from 2.331(6) to 2.514(6) Å. It is worth noting that the distances for Pb−O1, Pb−O4, Pb−O5, and Pb−O8 in the range of 3.028(5), 2.914(6), 2.880(6), and 3.034(6) Å are all shorter than the sum of the van der Waals radii (<3.1 Å), indicating the strong secondary interaction between the Pb(II) ion and the O atom.[17] This is also true for complex **15**. Both the coordination interaction and secondary interaction contribute to stabilization of the four-coordination sandwiched configuration of **3** and **15**. The two N_2O_2 planes of the Schiff-base ligands are approximately parallel, with a dihedral angle of 17.89(2)° for **3** and 12.57(7)° for **15**, respectively. These sandwich-type configurations for **3** and **15** are in line with the previous report of the Cu−Pb−Cu complex formed also with Schiff-base ligands.[18] Complex **4** exhibits a two-blade propeller-like structure, similar to **1** and **2**, and the two N_2O_2 planes of the L^b ligands are crossed with a dihedral angle of 78.74(5)°. As mentioned in the Experimental Section, after pure complex **4** was recrystallized from the mother solution, three single crystals of complex **15**, as a byproduct of **4**, were isolated from the concentrated filtrate. Unfortunately, further study on the luminescent properties of this complex was retarded due to its limited amount, since trials to get large amounts of **15** failed repeating the above-mentioned procedure. As a result, only the structure of **15** was undoubtedly revealed by single-crystal X-ray diffraction analysis.

Crystal Structures of $\{Nd[Zn(L^a)Cl]_2(H_2O)\}_2\cdot ZnCl_4\cdot 4H_2O$ (5), $\{Nd[Zn(L^b)Cl]_2(DMF)(OAc)\}\cdot CH_3CN$ (6), $[Eu(ZnL^a)_2Cl_2(H_2O)]\cdot 0.5ZnCl_4\cdot 2MeOH$ (7), $\{Eu[Zn(L^b)Cl]_2(DMF)(OAc)\}\cdot CH_3CN$ (8), $[Gd(ZnL^a)_2Cl_2\cdot H_2O]\cdot 0.5ZnCl_4\cdot 2MeOH$ (9), $[Gd(ZnL^b)_2Cl_2\cdot 2DMF]\cdot Cl\cdot 2H_2O$ (10), $[Tb(ZnL^a)_2Cl_2(H_2O)]\cdot 0.5ZnCl_4\cdot 2MeOH$ (11), $\{Tb[Zn(L^b)Cl]_2(DMF)_2\}\cdot Cl\cdot 2H_2O$ (12), $[Dy(ZnL^a)_2Cl_2(H_2O)]\cdot 0.5ZnCl_4\cdot 2MeOH$ (13), and $\{Dy[Zn(L^b)Cl]_2(DMF)_2\}\cdot Cl\cdot 2H_2O$ (14). As displayed in Figures S2−S4 (Supporting Information), complexes **5**, **7**, **9**, **11**, and **13** containing different M(III) metal ions are isostructural, possessing a two-blade propeller-like configuration, while complexes **6**, **8**, **10**, **12**, and **14** exhibit a sandwich-type configuration. Selected bond distances and angles for these complexes are listed in Table S2 (Supporting Information). Complexes **9** and **10** are taken as typical representatives to illustrate the molecular structure for these complexes in detail. As shown in Figure 4, **9** and **10** are formed by changing the central metal from Cd(II) for **1** and **2** to Gd

(17) (a) Soudi, A. A.; Marandi, F.; Morsali, A.; Zhu, L.-G. *Inorg. Chem. Commun.* **2005**, *8*, 773. (b) Yuan, Y.-Z.; Zhou, J.; Liu, X.; Liu, L.-H.; Yu, K.-B. *Inorg. Chem. Commun.* **2007**, *10*, 475.
(18) Thurston, J. H.; Tang, C. G.-Z.; Trahan, D. W.; Whitmire, K. H. *Inorg. Chem.* **2004**, *43*, 2708.

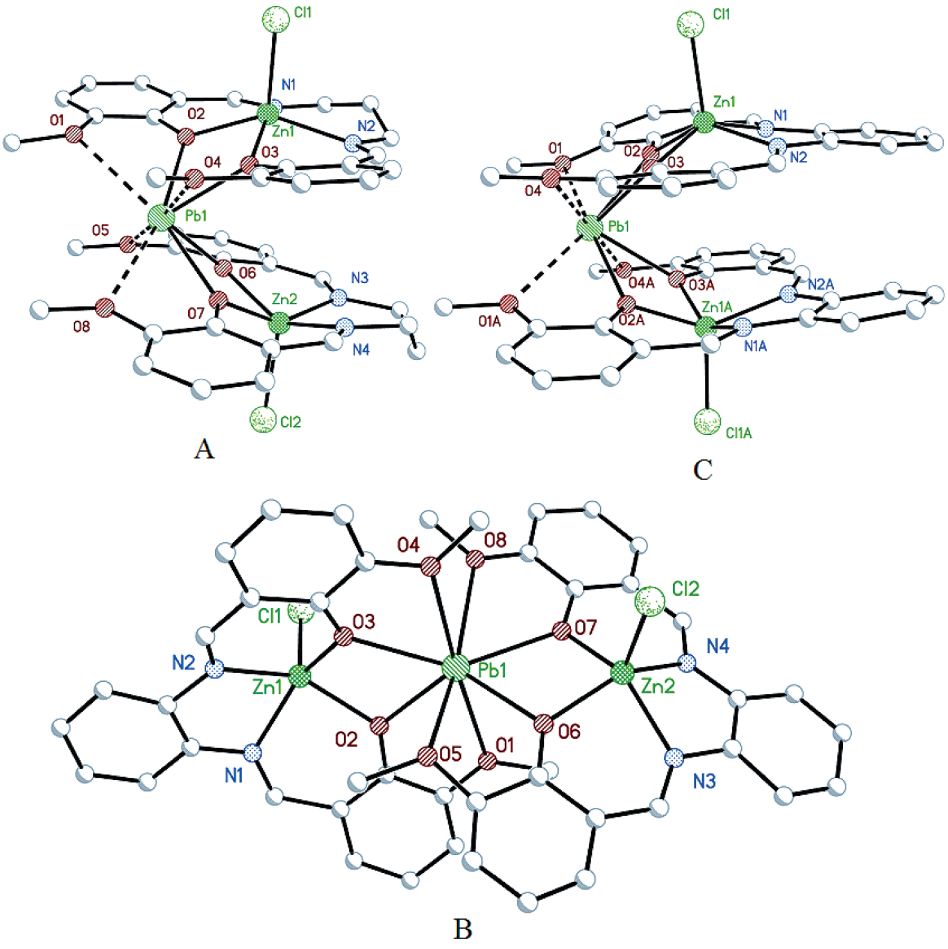

Figure 3. ORTEP drawings for compounds **3** (A), **4** (B), and **15** (C), with all H atoms and solvent molecules omitted for clarity.

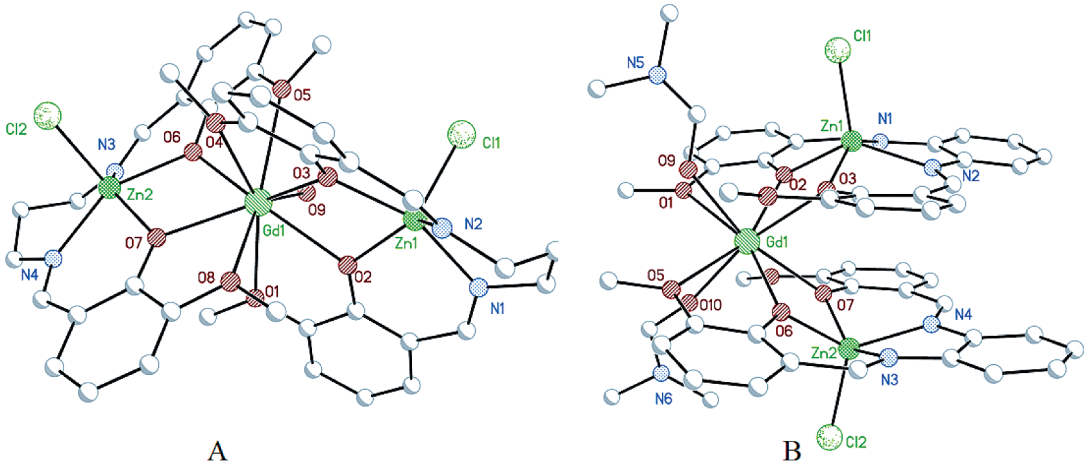

Figure 4. Structure diagrams of compounds **9** (A) and **10** (B) with all H atoms and solvent molecules omitted for clarity.

(III) for **9** and **10**. However, compound **9** exhibits a two-blade propeller-like configuration, absolutely different from the sandwich-type configuration of **10**, probably due to the different coordination preferences of the L (L = L^a and L^b) ligand in these two complexes. In detail, compound **9** belongs to the space group *Pbcn* and consists of one $\{Gd[Zn(L^a)Cl]_2(H_2O)\}^+$ cation, half a $ZnCl_4^{2-}$ anion, and two methanol molecules of crystallization in the asymmetric unit. The $\{Gd[Zn(L^a)Cl]_2(H_2O)\}^+$ motif is constructed from two $[Zn(L^a)Cl]^-$ units with a bridging Gd(III) ion. In comparison with complexes **1**, **2**, and **4**, the chiralilty of the $\{Gd[Zn(L^a)Cl]_2(H_2O)\}^+$ unit is not destroyed by the coordination number of the central Gd ion in **9**. The two enantiomers of complex **9** depicted as a left-handed and right-handed configuration are shown in the Figure 5. The Gd−O bond distances fall in the range of 2.311(2)−2.620(2)Å in **9**; the Zn(II) and Gd(III) ions are separated at distances of Zn1−Gd1 = 3.571(2) Å and Zn2−Gd1 = 3.634(2) Å.

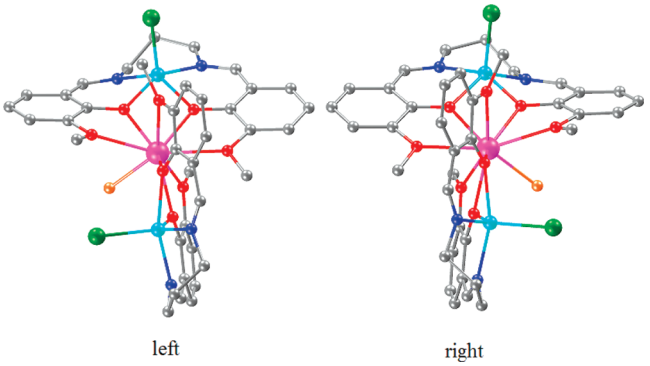

Figure 5. Drawings of two enantiomers $[M(ZnL^a)_2H_2O]^+$ in complexes **5**, **7**, **9**, **11**, and **13**.

All of these distances are comparable to those reported previously for dinuclear Schiff-base complexes.[19] The N_2O_2 planes of salen ligands are crossed with a dihedral angle of 83.70°, and the Zn1−Gd1−Zn2 angle is 179.56(10)°. This is also true for **5**, **7**, **11**, and **13**.

Compound **10** belongs to the space group $P2_1/n$ and possesses a sandwich-type configuration. It is noteworthy that a similar structure was observed for a similar complex, Zn−Nd−Zn.[8c] However, the coordination environment for the central metal ion is different. In the present case, the metal center Gd ion is coordinated by eight oxygen atoms, six from two ZnL^b units and two from two solvent DMF molecules. The Gd−O bond lengths span the range of 2.282(10)−2.758(8) Å, similar to those in other Schiff-base complexes involving the Gd(III) ion.[20] The distances of Zn1−Gd1 and Zn2−Gd1 are 3.534(8) and 3.513(8) Å, respectively. The Zn1−Gd1−Zn2 angle is 91.93(3)°, and the dihedral angle of the N_2O_2 planes from two L^b ligands is 18.61(3)°. This is also true for **12** and **14**. However, despite the sandwich-type configuration also employed by complexes **6** and **8**, the coordination environment for the central metal ion is different. The central metal ion Nd(III) or Eu(III) in **6** and **8** is coordinated with nine oxygen atoms, six from two ZnL^b units, one from the solvent DMF molecule, and two from the bidentate chelating acetic group, Figure S2 (Supporting Information).

IR Spectra. In the IR spectra of mononuclear Zn(II) Schiff-base complexes, the absorption bands at 1628 and 1220 cm^{-1} for ZnL^a and 1613 and 1237 cm^{-1} for ZnL^b are attributed to the C=N and C−N stretching vibrations of Schiff-base ligands, respectively. In addition, a strong absorption appears at 738 and 736 cm^{-1} for complexes ZnL^a and ZnL^b, respectively, which is assigned to the C−H bending vibration of benzene rings. It is worth noting that, despite the further complexation of the oxygen atoms in ZnL^a or ZnL^b with the central metal ion, there appears to be no obvious shift for these characteristic absorption bands in the IR spectra of trinuclear complexes **1**−**14**, in comparison with those of ZnL^a or ZnL^b. It is worth noting that observation of the absorption band at about 1652 cm^{-1} in the IR spectra of complexes **6** and **8** indicates the existence of a coordinated carboxylic group.

Electronic Absorption Spectra. The electronic absorption spectra of the two mononuclear complexes ZnL^a and ZnL^b and trinuclear complexes **1**−**14** in DMSO were recorded, and the data are compiled in Table 4. As shown in Figure S5 (Supporting Information), two absorption bands at 286 and 368 nm due to the $\pi-\pi^*$ transitions of the Schiff base ligand are observed for ZnL^a.[8c,13,21] With the spacer changing from *N*,*N*′-bis(3-methoxy-salicylidene)propylene-1,3-diamine for L^a to *N*,*N*′-bis(3-methoxysalicylidene)-benzene-1,2-diamine for L^b, as expected, the two absorptions of ZnL^b are red-shifted to 311 and 415 nm, respectively, due to the more extended conjugated system of L^b compared to that of L^a, Table 4 and Figure S6 (Supporting Information). The formation of trinuclear complexes with either a propeller or sandwich configuration from two ZnL^a or ZnL^b segments with the help of additional metal ions does not induce a significant change in the electronic absorption spectra. As shown in Figure S7 (Supporting Information), in comparison with ZnL^a, the higher-energy absorption band of trinuclear species **1**, **3**, **5**, **7**, **9**, **11**, and **13** containing a ZnL^a subunit remains almost unchanged at 285−287 nm, while the lower-energy absorption slightly blue-shifts to 347−352 nm. This is also true for trinuclear complexes of **2**, **4**, **6**, **8**, **10**, **12**, and **14** containing the ZnL^a subunit, regardless of their molecular configuration, Figure S6 (Supporting Information).

Luminescent Properties. The fluorescence spectra of ZnL^a, ZnL^b, and the whole series of Zn−M−Zn trinuclear complexes **1**−**14** have been recorded both in solution and in the solid state at room temperature, and the related data are also organized in Table 4. As can be seen, the solution emission spectra of complexes ZnL^a and ZnL^b are very similar and could be assigned to typical intraligand emission.[21] The emission band was observed at 483 and 544 nm, respectively, for ZnL^a and ZnL^b. The red shift of the emission peak of ZnL^b in comparison with that of ZnL^a is attributed to the extended conjugated system of ZnL^b due to the aromatic bridge.[13,21]

Coordination of the oxygen atoms in ZnL^a or ZnL^b with the central metal ions with a different charge and ionic radius leads to different luminescent properties for trinuclear complexes **1**−**14**. As shown in Figure S8 (Supporting Information), complexes **1**, **3**, **7**, **9**, **11**, and **13** show a broad emission band with a maximum peak in the region of 453−463 nm in DMSO. The fluorescence lifetimes of these emissions are similar to that of ZnL^a, revealing the ligand-originated nature of these emissions. These bands take a blue shift of 20−30 nm relative to the intraligand emission band at 483 nm for mononuclear precursor ZnL^a, probably due to the electron-withdrawing effect of the central metal ion. However, the broad emission band at 542−544 nm for trinuclear complexes **2**, **4**, **8**, **10**, **12**, and **14** does not show a significant shift in comparison with that of ZnL^b at 544 nm, Figure S9 (Supporting Information), indicating a lesser disturbance

(19) (a) Connor, J. A.; Charlton, M.; Cupertino, D. C.; Lienke, A.; McPartlin, M.; Scowen, I. J.; Tasker, P. A. *J. Chem. Soc., Dalton Trans.* **1996**, 2835. (b) Raquel, R. C.; Fernando, A.; Carlos, O. L.; Daniel, I.; Bunzli, J.-C. G.; Andres de, B.; Teresa, R. B. *Inorg. Chem.* **2002**, *41*, 5336.

(20) (a) Kido, T.; Ikuta, Y.; Sunatsuki, Y.; Ogawa, Y.; Matsumoto, N. *Inorg. Chem.* **2003**, *42*, 398. (b) Madalan, A. M.; Avarvari, N.; Fourmigue, M.; Clerac, R.; Chibotaru, L. F.; Clima, S.; Andruh, M. *Inorg. Chem.* **2008**, *47*, 940. (c) Kido, T.; Nagasato, S.; Sunatsuki, Y.; Matsumoto, N. *Chem. Commun.* **2000**, 2113.

(21) Lo, W.-K.; Wong, W.-K.; Wong, W.-Y.; Guo, J.; Yeung, K.-T.; Cheng, Y.-K.; Yang, X.-P.; Jones, R. A. *Inorg. Chem.* **2006**, *45*, 9315.

Table 4. Data of UV Absorptions in DMSO (10^{-5} M) Solution and Emissions in Solution and Solid State

	abs, λ_{max}/nm, [log(ε/dm^3 mol^{-1} cm^{-1})]	excitation in solution, λ_{ex}/nm	emission at 298 K for solution, λ_{em}/nm (τ, $10^3\Phi_{em}$)	excitation in solid, λ_{ex}/nm	emission at 298 K in solid state, λ_{em}/nm
ZnL[a]	286 (3.96), 368 (3.91)	285, 360	483 (0.71 ns, 5.3)	385	518
ZnL[b]	311 (4.13), 415 (4.02)	460	544 (0.34 ns)	460	569
1	287 (4.13), 357 (4.11)	285, 360	462 (0.86 ns, 2.72)	385	465
2	306 (4.27), 342 (4.19), 402 (4.14)	460	542 (0.38 ns, 1.03)	460	554
3	287 (4.03), 356 (3.86)	285, 360	460 (0.72 ns, 3.58)	385	467
4	306 (4.07), 340 (4.26), 396 (4.03)	460	544 (0.29 ns, 3.45)	460	558
5	286 (4.21), 351 (4.05)	285, 360	474 (0.85 ns, 0.20 ns, 2.33), 876, 1064 (1.27 μs), 1352	385	491, 876,1064, 1084, 1352
6	305 (4.44), 340 (4.36), 391 (4.12)	460	543 (0.24 ns, 0.054 ns, 6.30), 876, 1064 (1.12 μs), 1352	460	545, 876, 1064, 1084, 1352
7	285 (4.38), 348 (4.18)	285, 360	453 (0.72 ns, 3.08)	385	456
8	306 (4.20), 341 (4.11), 397 (3.90)	460	542 (0.92 ns, 5.41)	460	546
9	286(4.29), 347(4.03)	285, 360	453 (0.73 ns, 4.01)	385	448
10	306 (4.20), 339 (4.10), 395 (4.02)	460	543 (0.68 ns, 3.43)	460	544
11	286 (4.39), 351 (4.11)	285, 360	463 (0.74 ns, 0.16 ns, 5.18), 489, 543	385	489, 543, 547, 586, 626
12	3.06 (4.32), 340 (4.13), 395 (3.92)	460	542 (0.32 ns, 4.45)	460	543
13	285 (4.40), 348 (4.13)	285, 360	463 (0.82 ns, 1.91)	385	482, 565, 578, 667
14	306 (4.32), 338 (4.23), 395 (4.07)	460	543 (0.64 ns, 5.31)	460	545

of the coordination of ZnL[b] with the central metal ion at the energy levels of the excited states of ZnL[b].

In addition to the wide intraligand emission in the region of 400−650 nm, trinuclear complex **11** (Tb with ZnL[a] precursor) exhibits extra sharp emission peaks at 489 and 543 nm in DMSO, corresponding to the emission of the Tb(III) ion and indicating the energy transfer from ligands to the Tb(III) ion, Figure 6. However, observation of the remnant intraligand emission at 400−650 nm for this compound suggests that the energy transfer is less efficient. Otherwise, this emission from the ligands will be completely quenched. It is worth noting that, in addition to the lifetime attributed to the intraligand emission, 0.74 ns, another quicker decay for the excited state of **11** with a lifetime of 0.16 ns was also revealed by the lifetime measurement and is assigned to the energy transfer from the ligands to the central metal ion. In contrast, typical emissions of the Eu(III) and Dy(III) ions in **7** and **13** were not observed, indicating the absence of energy transfer from the ligands to the metal ion in these complexes. It is well-known that efficient energy transfer between a donor and an acceptor requires a large overlap between the emission of the donor and the absorption of the acceptor. The absence of an energy transfer from the ligands to the central rare earth metal ion for **7** and **13** is therefore most probably due to the fact that the energy levels of the ZnL[a] emission do not match with the absorption of Eu(III) and Dy(III) ions. This is also true for the trinuclear complexes **8** (Eu), **12** (Tb), and **14** (Dy) formed from the ZnL[b] precursor. However, in addition to the normal intraligand emission band at 543 nm, sharp multiple emission peaks in the near-IR region corresponding to the emission from the Nd(III) ion were observed in the fluorescence spectrum of **6** in DMSO. The emission band centered at 876 nm was assigned to the transition of $^4F_{3/2}$−$^4I_{9/2}$, whereas the band at 1064 nm was assigned to $^4F_{3/2}$-$^4I_{11/2}$ and that 1352 nm to $^4F_{3/2}$−$^4I_{13/2}$, Figure 7. The lifetime of these near IR emissions was revealed to be 1.12 μs, corresponding well with that of Nd(III) according to a

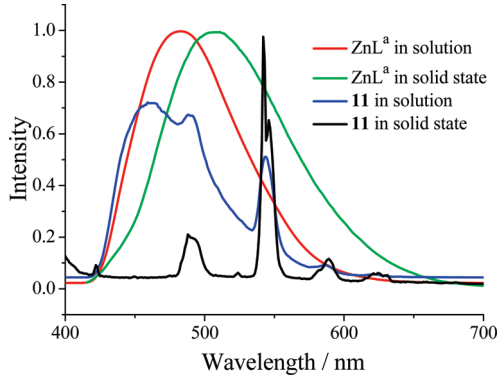

Figure 6. Emission spectra of complexes ZnL[a] and **11** in DMSO solution and the solid state.

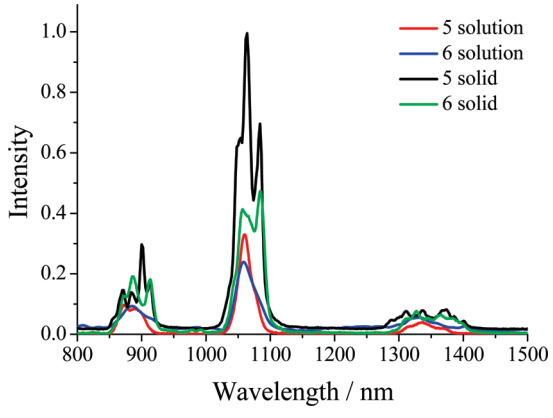

Figure 7. Emission spectra of complexes **5** and **6** in DMSO solution and the solid state.

previous report.[21] In line with the result for **11**, observation of the emissions due to the Nd(III) ion in the near-IR region indicates the energy transfer from the ligand to Nd (III) in **6**. As organized in Table 4, two fluorescence lifetimes, 0.24 and 0.057 ns, were recorded for the emissions of **6** in the visible region, with the former one corresponding to the normal intraligand emission and the latter one to the energy transfer from ZnL^b to Nd(III). As expected, very similar fluorescence properties have been revealed for the Nd analogue **5** formed with the ZnL^a precursor, Figure 7 and Table 4. It is worth noting that the luminescence properties result of the present trinuclear Schiff-base complexes is in line with that of their binuclear analogues reported previously: Efficient energy transfer between the ligand and the central metal ion exists in some complexes of rare earth metals, such as Nd(III), but does not exist in some complexes of rare earth metals, such as Er(III) and Gd(III).[21] An unambiguous explanation for this phenomenon is still not clear at this stage but is most probably due to the difference in the electronic and molecular structures of different complexes associated with different rare earth metals and Schiff-base ligands.

The solid-state emission spectra of complexes **1**−**14** together with those of the two precursors ZnL^a and ZnL^b have also been recorded at room temperature, Table 4. As shown in Figures S10 and S11 (Supporting Information) as well as in Table 4, similar to their manners in DMSO solution, trinuclear complexes **1**, **2**, **3**, **4**, **7**, **8**, **9**, **10**, **12**, and **14** display a broad emission band in the visible region due to the intraligand emission. No significant shift of the emission peak for these compounds in the solid state relative to that in solution was observed. However, a quite significant change was observed in the solid-state emission spectra of **5**, **6**, **11**, and **13** in comparison with those in solution. Unlike the presence of an intraligand emission band in the visible region for **11** in DMSO solution, in the solid-state emission spectrum of this compound, the intraligand emission disappears completely. As for **5**, **6**, and **13**, a relatively weakened intraligand emission in comparison with that in DMSO in the region of 400−550 nm was observed in their solid-state emission spectra. Nevertheless, a set of new sharp peaks at 482, 565, 578, and 667 nm attributed to the emission of the Dy(III) ion, which are not observed in the solution spectrum, appear in the solid-state emission spectrum of **13**. These results reveal the enhanced energy transfer from the ligand to the rare earth ion in the solid state compared to that in DMSO solution.

It is also worth noting that, in DMSO solution, the emission peaks of complex **5** at 876 nm ($^4F_{3/2}$−$^4I_{9/2}$) and 1068 nm ($^4F_{3/2}$−$^4I_{11/2}$) are sharp peaks without hyperfine structure, Figure 7. However, in the solid state, these peaks split into two or more sharp peaks, revealing the low-symmetry coordination environment around the central metal ion in the solid state, which was disturbed by the salvation effect in solution.[22] A similar peak splitting has also been observed for the rare earth ion emission peaks of **6**, **11**, and **13** in their solid state spectra.

Conclusion

A series of 15 phenoxo-bridged trinuclear Schiff-base complexes have been assembled on the basis of two symmetrical Schiff-base ligands in a step-by-step method. X-ray diffraction analysis reveals that eight complexes are comprised of chiral enantiomers, in which two screwed five-coordinated Zn(II) segments, ZnL (L = L^a and L^b), embrace the central metal ion, forming the chiral two-blade propeller-like left-handed and right-handed Zn−M−Zn configuration. The other seven complexes exhibit a sandwich-type molecular structure. Comparative and systematic investigation of the photophysical properties of these trinuclear complexes reveals that the luminescence properties could easily be tuned by changing the central metal or the Schiff-base ligand.

Acknowledgment. This work was supported by the National Natural Science Foundation of China and the Postdoctoral Scientific Foundation of China (Nos. 200704211076 and 200801414).

Supporting Information Available: Structure diagrams of two enantiomers in complex **1**; ORTEP drawing of the structures of compounds **5**, **7**, **11**, and **13** (M = Nd, Eu, Tb, and Dy); ORTEP drawings of the structures of complexes **6** and **8** (M = Nd and Eu); ORTEP drawing of the structures of complexes **12** and **14** (M = Tb and Dy); electronic absorption, excitation (monitored at 483 nm), and emission spectra of ZnL^a in DMSO and the solid state; electronic absorption spectra of complexes ZnL^b, **2**, **4**, **6**, **8**, **10**, **12**, and **14** in DMSO; electronic absorption spectra of complexes **1**, **3**, **5**, **7**, **9**, **11**, and **13** in DMSO; emission spectra of complexes ZnL^a, **1**, **3**, **7**, **9**, **11**, and **13** in DMSO (λ_{ex} = 285 nm); emission spectra of complexes **2**, **4**, **8**, **10**, **12**, and **14** in DMSO (λ_{ex} = 460 nm); emission spectra of complexes **1**, **3**, **7**, **9**, 11, and **13** in the solid state (λ_{ex} = 385 nm); emission spectra of complexes ZnL^b, **2**, **4**, **8**, **10**, **12**, and **14** in the solid state (λ_{ex} = 460 nm); crystal data and structure refinement for complex **15**; and selected bond lengths (Å) and angles (deg) of complexes **5**−**8** and **11**−**14**. This material is available free of charge via the Internet at http://pubs.acs.org.

(22) (a) Geng, F.; Matsushita, Y.; Ma, R.; Xin, H.; Tanaka, M.; Izumi, F.; Iyi, N.; Sasaki, T. *J. Am. Chem. Soc.* **2008**, *130*, 16344. (b) Bazzi, R.; Flores-Gonzalez, M. A.; Louis, C.; Lebbou, K.; Dujardin, C.; Brenier, A.; Zhang, W.; Tillement, O.; Bernstein, E.; Perriat, P. *J. Lumin.* **2003**, *102*, 445. (c) Lakshminarayana, G.; Yang, H.; Teng, Y.; Qiu *J. Lumin.* **2009**, *129*, 59.